

Remote Steering of Self-Propelling Microcircuits by Modulated Electric Field

Rachita Sharma and Orlin D. Velev*

The principles and design of “active” self-propelling particles that can convert energy, move directionally on their own, and perform a certain function is an emerging multidisciplinary research field, with high potential for future technologies. A simple and effective technique is presented for on-demand steering of self-propelling microdiodes that move electroosmotically on water surface, while supplied with energy by an external alternating (AC) field. It is demonstrated how one can control remotely the direction of diode locomotion by electronically modifying the applied AC signal. The swimming diodes change their direction of motion when a wave asymmetry (equivalent to a DC offset) is introduced into the signal. The data analysis shows that the ability to control and reverse the direction of motion is a result of the electrostatic torque between the asymmetrically polarized diodes and the ionic charges redistributed in the vessel. This novel principle of electrical signal-coded steering of active functional devices, such as diodes and microcircuits, can find applications in motile sensors, MEMs, and microrobotics.

1. Introduction

The science of complex functional particles is expanding rapidly toward new types of “active” motile and self-propelling particles.^[1–6] These particles usually carry a certain amount of propellant compound and catalyze or convert the chemical or field energy from their environment into controlled directional motion. Novel techniques for making propelling particles, a few millimeters or smaller in size, are being actively explored. Some examples include Marangoni effect driven by temperature or concentration gradients,^[7–9] bubble propulsion through catalytic decomposition of chemical “fuel,”^[10–12] self-electrophoresis using coupled redox reactions,^[13–15] diffusiophoresis resulting from concentration gradient around particles,^[16,17] application of self-oscillatory reactions such as the Belousov–Zhabotinsky reaction,^[18,19] integration of biological and synthetic components to create hybrid motile particles,^[20,21] and application of external electric fields,^[22–24] magnetic fields^[25,26] and ultrasound^[27,28] to generate motion. It can be hypothesized that in

the not-so-distant future this research evolution will result in new types of “smart” particles that could move on their own, sense and respond in highly specific ways to stimuli from their environment.^[29–39]

We have introduced previously a class of motile particles based on miniature semiconductor diodes powered by a global uniform alternating (AC) electric field.^[24] The millimeter-sized diodes float on water and are subjected to an external AC field applied via remotely positioned electrodes. The particle-localized electroosmotic (EO) flux, resulting from the DC voltage rectified by the diodes, propels them in a direction determined by the diodes’ orientation and surface charge (Figure 1a). Importantly, their velocity was found to be independent of field frequency and diode size, which suggests that the moving microcircuits can poten-

tially be powered by contactless radio and microwave emitters. These principles of providing power remotely through AC fields open possibilities of making “self-propelling” microdevices, which we define as ones capable of harvesting energy from external sources and rectifying and converting it into directional hydrodynamic propulsion. We demonstrated that such self-propelling diodes can also have complex functionalities. For example, light emission along with propulsion was demonstrated by light-emitting diodes (LEDs), and in more complex devices a rotor ring with LEDs attached on its periphery exhibited rotational motion by harnessing the external uniform AC electric field. Diodes immobilized on the walls of microfluidic channels were shown to pump and mix liquids.^[40] The principle has been extended to the microscale by Wang et al., by showing how semiconductor diode nanowires can be propelled by the principle of AC electric field rectification.^[41] More recently, Roche et al. developed electronic swimmers (“e-swimmers”) based on bubble-propulsion resulting from electric-field induced polarization, and demonstrated complex functionalities (such as light emission) powered by the localized electric current in the swimmers.^[42]

The next breakthrough in this research is developing means of steering the moving microdevices. The direction of electroosmotic flux near the diode surface is always toward the electrode with DC bias opposite to the counterionic charge, regardless of the diode orientation (Figure 1a). The ability to remotely rotate the orientation of the self-propelling diode would make possible its steering and unlimited motion by on a controlled

Dr. R. Sharma, Prof. O. D. Velev
Department of Chemical and
Biomolecular Engineering
North Carolina State University Raleigh
NC 27695-7905, USA
E-mail: odvelev@ncsu.edu



DOI: 10.1002/adfm.201502129

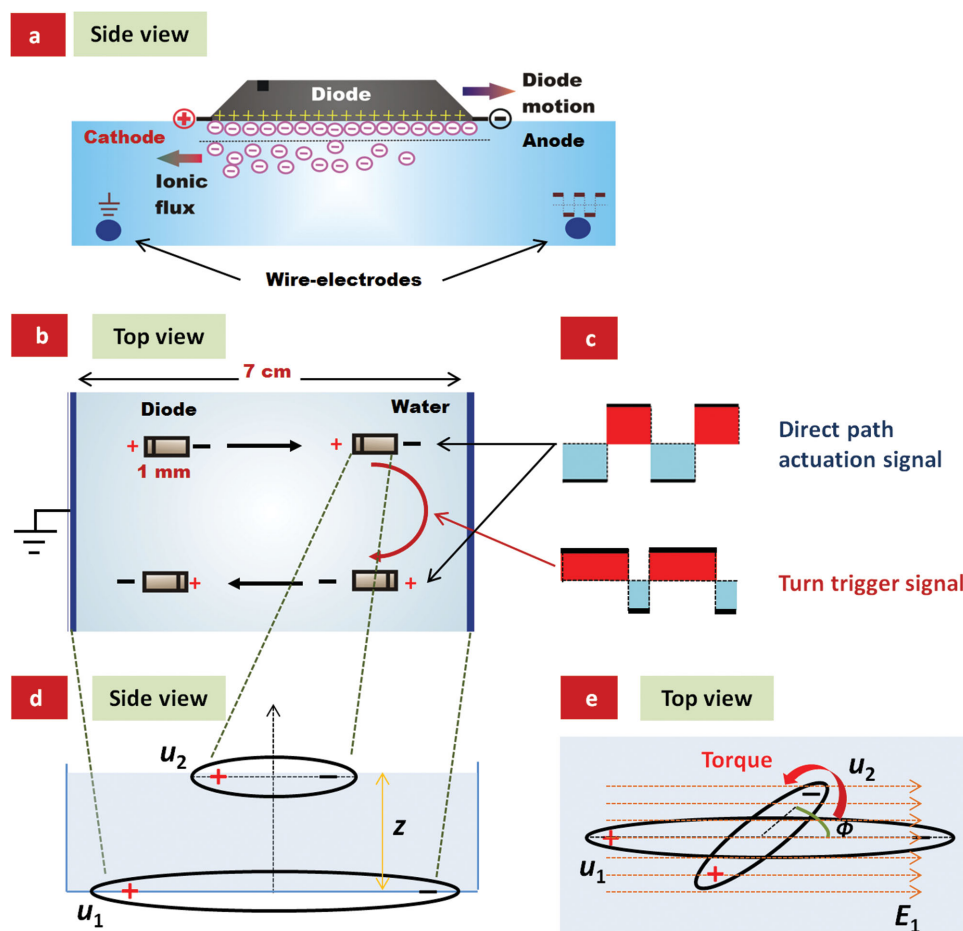


Figure 1. a) Schematic illustrating the mechanism of self-propulsion of a diode floating on water. The direct (DC) potential developed across the diode from the rectified AC field propels the microdevice by electroosmosis (see ref.^[24]). b) Schematic of the process of diode turnaround and c) types of AC signal used to actuate the diode motion and trigger its turn in this work. d) Side view and e) top view of the dipole model for the torque emerging during the application of the asymmetric signal in (c) leading to the turn. The charged diode (represented as dipole u_d) is rotating under the influence of the redistributed counterions in the vessel (represented as dipole u_c), going from unfavorable orientation (parallel dipoles) to favorable orientation (antiparallel dipoles).

trajectory.^[24] We present here a novel technique that allows us to perform such steering electronically. The diodes rotate and reverse their direction of motion when a wave asymmetry (equivalent to a DC voltage offset) is introduced into the AC signal providing them with energy (Figure 1b). In addition to back and forth motion, the diodes can be moved sideways (at an angle) through certain wave symmetry modulations. This phenomenon is unique to devices such as diodes that have asymmetric electrical conductance. We describe the phenomenology and perform a brief analysis of the complex physical origins of these electrohydrodynamic effects.

2. Results and Discussion

2.1. Origin of the Propulsion and Effect of a Constant DC Field on Diode Dynamics

In the experimental setup, millimeter-sized commercial microcircuit diodes are freely floating suspended by capillarity

over the surface of water contained in a Petri dish. Electric fields are applied through two wire electrodes extended across the bottom of the water container (Figure 1a and the Experimental Section). When a uniform external AC field is applied to the electrodes, the self-propelling diode experiences only an electric polarization torque that aligns it in the direction of the field (regardless of which direction the diode is facing).^[24,43] The DC potential drop across the diode always points in the direction of its anode (as illustrated in Figure 1b) and hence, it always follows the orientation of the diode (unlike the case of particles from isotropic material such as polymer).

A DC electric field component added to the external AC signal would induce an additional rotational torque on the diode due to the interaction of the induced DC field across the diode and the DC offset applied across the electrode gap. We can relate this effect to the physical origins of the dipole-dipole interactions. The normalized energy of interaction, W , between two dipoles of dipole moments u_1 and u_2 aligned in parallel planes (Figure S1, Supporting Information) can be estimated by

$$\frac{w}{\left(\frac{u_1 u_2}{4\pi\epsilon_0\epsilon r^3}\right)} = W = \cos\phi \quad (1)$$

where w is the interaction energy, ϵ_0 is the permittivity of free space, ϵ is the relative dielectric permittivity of the medium, r is the distance between the centers of the two dipoles, and ϕ is the rotation angle defining the alignment of one dipoles with respect to the other.^[44] The two dipoles prefer to orient antiparallel in relation to each other as the dipole–dipole interaction energy is minimized in this configuration, whereas the interaction energy is maximal (unfavorable) in parallel orientation (Figure S1, Supporting Information). Analogously, the diode would prefer to align such that the DC field induced by the AC signal rectification is oriented antiparallel to an external DC field component. We can also interpret this effect as the tendency of a diode to align itself in forward bias with respect to the DC field, as its polarizability is highest and the energy is minimal in this orientation.

The problem of controlling and changing the direction of diode motion thus can be solved by imparting a torque on the diode by an external DC field. Direct continuous application of a DC field across the vessel, however, is rather problematic, because of the EO flows originating near the Petri dish surface (Figure S2, Supporting Information). These macroscopic flows are very undesirable, as they significantly disrupt the diode motion and rotation by drifting it forward or backward depending on the direction of the external DC field. These unwanted EO flows can be minimized by adjusting the pH of the liquid to the isoelectric point (IEP) of the Petri dish surface (as done in the experiments aimed at analyzing the mechanism of the effect described in the next section). However, such fine-tuning of the experimental conditions would drastically limit the applicability of this technique. Therefore, we introduced an alternative versatile electronic signal-symmetry-coded control described in the next section.

2.2. Effect of Time-Lapsed DC Field on Diode Motion

A DC component can be introduced into an AC signal by changing the wave symmetry, also called duty cycle. We found out that the best approach of inducing a rotational torque on the diode, while avoiding the undesirable effects of a constant external DC component, is to apply a short-duration shift of the AC field wave symmetry leading to an intermittent DC component that creates a dipolar polarization in the vessel and indirectly causes the diode to respond and turn around (Figure 1b,c). This technique was implemented by introducing a capacitor in series with the wire electrodes (the circuit scheme is given in Figure 5 in the Experimental Section). The capacitor filters out the DC component of the signal once charged (Figure S3, Supporting Information). Thus, the external DC-modulated signal acts on the system only during the short transient period of less than a few seconds while the capacitor charges, after which it gets suppressed (for details see Figure S4 in the Supporting Information).

This approach of using a capacitor to introduce a short-lasting change in the AC field symmetry allowed us to shuttle

the self-propelling diode back and forth on the water surface by promptly turning it around on-demand, while avoiding the perturbation in diode motion from EO flows arising near the Petri dish surface (present when no capacitor is used and asymmetric signal is applied). Microscopy snapshots of one double-turnaround cycle with timing are shown in Figure 2. Every time the symmetry of the signal is changed, the steadily moving diode first accelerates rapidly (“jerks”) in the original direction of motion, after which it slows down, rotates and reaches the same steady state EO velocity in the opposite direction. The forward–backward shuttling can be repeated indefinitely as long as the signal symmetry is changed at the right timing sequence. These fascinating turnaround and shuffling dynamics are illustrated in Video V1 in the Supporting Information.

The above sequence of events can be explained bearing in mind that the time-limited DC impulse leads to two electrokinetic effects in the experimental cell. The first one is a short-time global electroosmotic flux of water medium streaming along the vessel bottom toward the electrode of same polarity as the charge on the bottom. This EO flow is mentioned in the previous section; however, in the case of an external capacitor in the circuit it is very short lived and, as we demonstrate further down, inconsequential with regards to diode orientation.

The second effect is additional counterion build-up in the double ionic layer around the electrodes—in effect charging

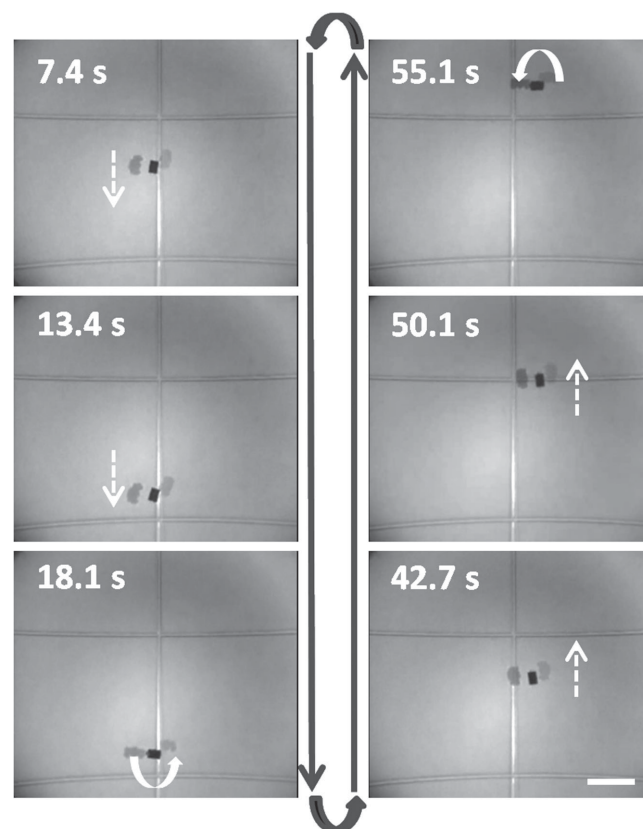


Figure 2. Time-lapse snapshots of a millimeter-sized diode floating on water and shuttling back and forth on-demand by introducing a short-duration DC component into the applied AC signal. The process is illustrated in Video 1 in SI. Scale bar = 5 mm.

of the two “electrolytic capacitors” formed by the two electrodes together with their counterionic atmospheres. Once the external DC component is eliminated by the capacitor, the counterion build-up across the wire electrodes has a strong indirect effect on the diode orientation. The field originating from the counterionic polarization is opposite in direction to the short-duration external DC field and can be considered as a large dipole superimposed along the length of the vessel (Figure 1d,e). Analogously to the dipole–dipole interactions described

in Section 2.1, the diode prefers to be aligned such that the DC field across it is antiparallel in relation to the counterionic field. If the diode faces in the opposite direction, the experimentally observed turnaround occurs. These sequential polarization processes, resulting in diode rotation, and the timed direction and velocity of the effect have been illustrated step by step in Figure 3.

In analyzing the series of effects described above, first we proved that the nonlinear electrical conductance of the diode

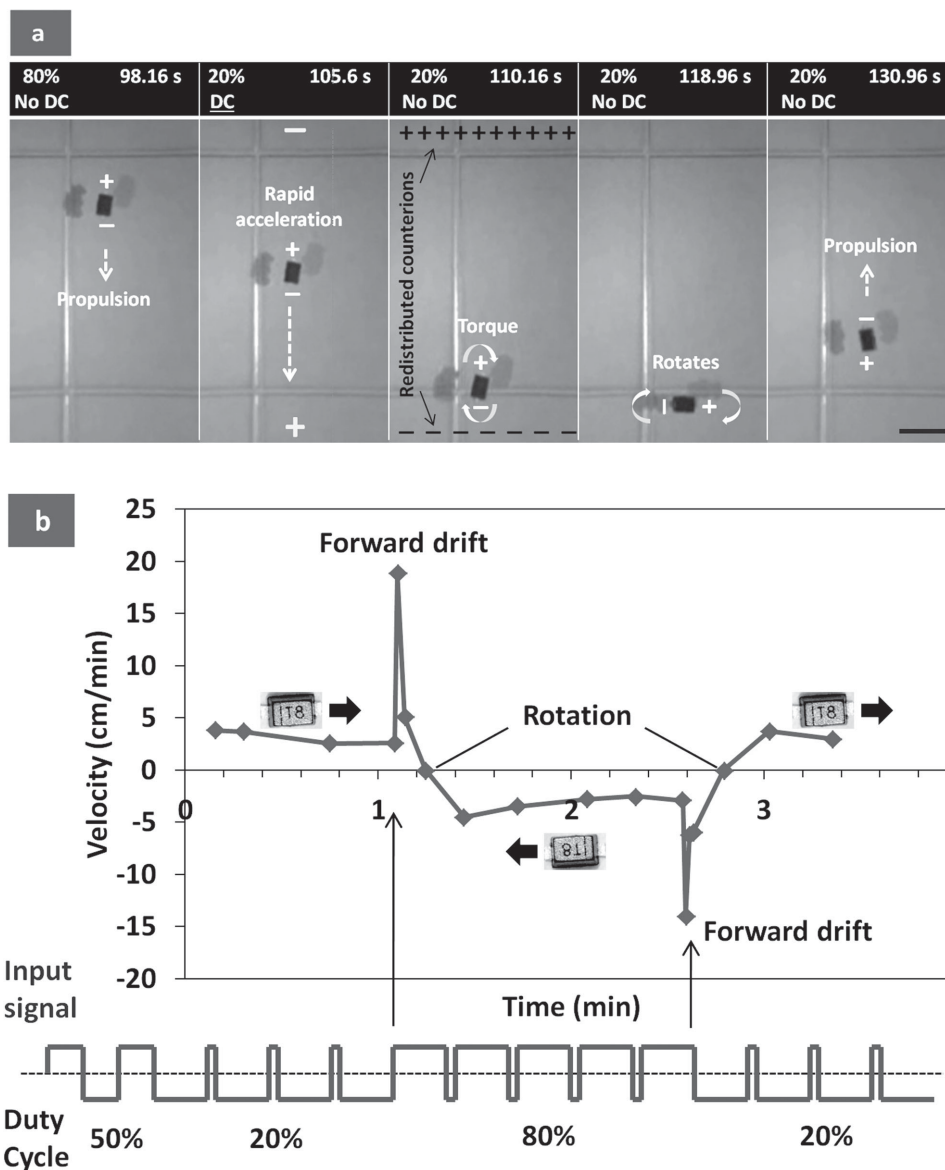




Figure 3. a) Time-lapse snapshots marked with the diode polarity and vessel polarization during the sequential process of rotation of a millimeter-sized diode on changing the duty cycle. During the short period right after changing the signal symmetry, when the capacitor is incompletely charged, the diode rapidly accelerates forward due to EO flows originating near the Petri dish surface. After the capacitor completely charges and the external DC component is blocked, the diode experiences torque from the field generated by the redistributed counterions and rotates in the reverse direction. Scale bar = 2 mm. b) Typical plot of velocity against time of a diode shuttling back and forth, along with a cartoon of the applied input signal. The rapid increase in diode velocity on changing the signal symmetry results from the transient electroosmotic flows in the Petri dish while the capacitor charges, following which the diode rotates due to the resulting counterion redistribution. The process can be repeated accurately as many times as desired.

Table 1. Summary of diode motion on water, for a given orientation with respect to wire electrodes, when the duty cycle of the AC signal is changed from 50% → 20% → 80% for driving circuits with capacitor (producing short-duration DC pulse) and without capacitor (constant DC signal component). The dynamics of diode motion are illustrated with arrows for each case. Experimental dynamics are shown in Video 3 in the Supporting Information.

Diode orientation		Without capacitor		With capacitor	
	50%	Propulsion	↑	Propulsion	↑
	20%	Tries to rotate (tilts, but no rotation) while drifting backwards	↓	i) short duration: tilts (no rotation) and stops ii) Aligns and keeps propelling	↑
	80%	Aligns again while drifting forwards	↑	i) Short duration: forward drift ii) Rotates and propels in opposite direction	↺
	50%	Propulsion	↓	Propulsion	↓
	20%	Rapidly accelerates (drifts) forward	↓	i) Short duration: forward drift ii) Rotates and propels in opposite direction	↻
	80%	Tries to rotate (tilts, but no rotation) while drifting backwards	↑	i) Short duration: forward drift ii) Rotates and propels in opposite direction	↺

is essential for the steering by replacing the diode with a piece of plastic of the same size and similar composition to the one of the diode. No rotation was observed when the floating particle was made of isotropic polymer and therefore did not exhibit a preference for one orientation over another in the presence of the counterionic field (Video V2, Supporting Information). The plastic piece only drifts forward–backward driven by the short-lasting EO flows arising near the Petri dish surface during capacitor charging, which also affect the diode as illustrated in Figure 3 and Figure S2 in the Supporting Information.

We next proved the critical role of the capacitor in the generation of a timed DC pulse that leads to ionic charging and polarization effects driving the diode turnaround. Table 1 summarizes the response of a self-propelling diode to a sequence of duty cycle changes applied with and without capacitor in the circuit and compares the two cases. The experimental dynamics for these two systems are seen in Video V3 in the Supporting Information. They prove the critical role of the capacitor for achieving transient DC torque and executing a turn. It should be noted that for a given change in AC signal symmetry, the DC voltage component at the wire electrodes when a capacitor was present in the circuit is up to two times higher than when no capacitor was present (Figure S3, Supporting Information).

The dynamics of the propelling diodes described above is a combination of transient charging effects driven by field asymmetry and the more trivial electroosmotic effects of fluid motion in the dish. In the final round of proof-of-mechanism experiments, we demonstrated that these two effects can be separated and characterized independently. When the pH of water was lowered to the IEP of the Petri dish, rapid acceleration of the diode was not observed prior to rotation due to

suppression of the EO flows in the vessel. Rotation was, however, still observed as counterion charging of the double layer around the wire electrodes still takes place. Similarly, when the pH was increased to the IEP of diode surface, diode self-propulsion was selectively inhibited in the absence of net ionic flux near the diode surface,^[24] while it continued to respond to the short-duration DC field and the resulting counterion redistribution and rotate in place (see Video V4 in the Supporting Information). The data proving that the signal-induced rotation is pH-independent lead to the key conclusion that while the diode motion itself is dependent on surface ionization and ionic charge, the signal-coded rotation is entirely a field-driven ionic polarization effect. A more detailed analysis of this effect is presented in the following section.

2.3. Theoretical Evaluation of the Torques on Diode

We estimated the rotational torque acting on the diode from the counterion redistribution, and the dipolar charge needed to achieve rotation at the rate observed in the experiment. This includes evaluations of the alignment torque and drag torque (details discussed in the Supporting Information). Drawing analogy to the dipole–dipole interactions (Figure 1d,e and Figure S1 in the Supporting Information), the rotational torque on the diode was evaluated by assuming it to be a finite dipole experiencing the field from counterion redistribution between the wire electrodes (Figure S5, Supporting Information). The field E_1 by the counterionic dipole was assumed to be equal the external DC field across the wire electrodes before the capacitor charges and blocks the external DC component ($E_1 = 6857 \text{ V m}^{-1}$). Assuming a steady-state motion, the rotational torque on the diode is balanced by the viscous drag

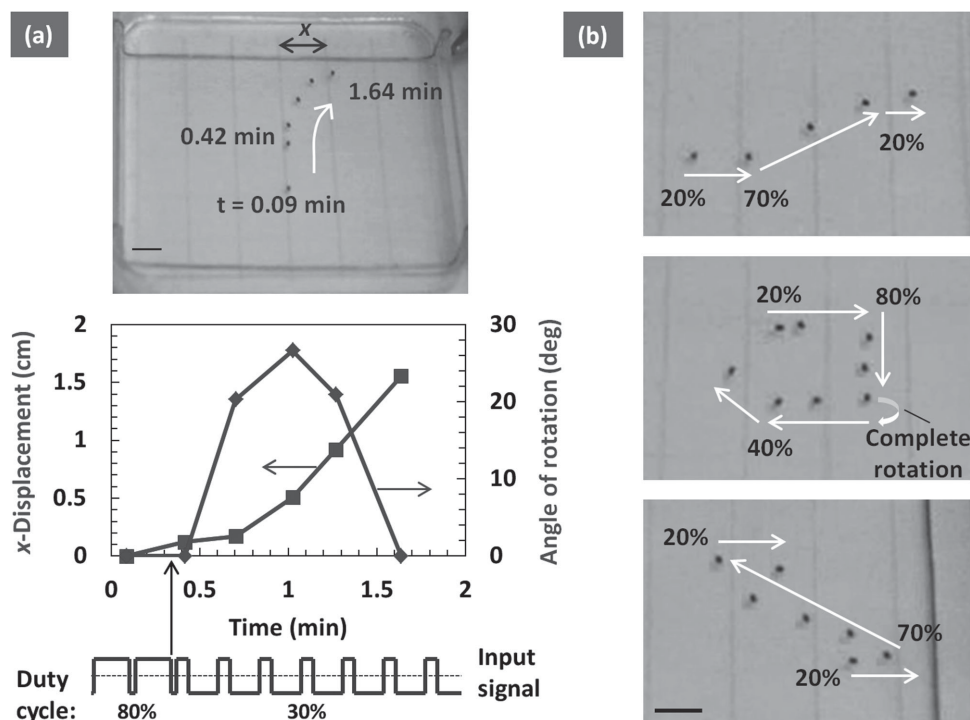


Figure 4. a) Photographic overlay of the trajectory of a self-propelling diode moving sideways (assembled from superimposed images), along with a plot of its x-displacement and angle of rotation versus time, when the duty cycle of the applied AC signal was changed from 80% \rightarrow 30% as shown in the cartoon of the input signal. b) Photographs of some of the more complex trajectories steered via sideways diode motion (assembled from superimposed images). Scale bars = 5 mm.

torque ($\tau_d = 1.83 \times 10^{-12}$ Nm) and the alignment torque from the external field ($\tau_a = 3.8 \times 10^{-12}$ Nm). We expressed the rotational torque τ_r on the diode, from the field of the counterionic dipole, as a function of the charge in the diode dipole q_2 ($\tau_r = 1.19 \times q_2$ Nm). Thus, we estimated the charge in the diode dipole q_2 to be $\pm 4.73 \times 10^{-12}$ C (more details are presented in the Supporting Information).

The related charge near the diode surface, evaluated on the basis of the Guoy–Chapman theory,^[44] came out to be $\pm 1.3 \times 10^{-10}$ C. Separately, we calculated the capacitive charge in the diode dipole, based on the internal diode capacitance specified by the manufacturer, as $\pm 2.4 \times 10^{-11}$ C. Since the actual charge in the diode dipole is larger than the charge required for the rotational torque to balance the drag and alignment torques, the actual rotational torque acting on the diode would be sufficient to rotate the diode by overcoming the drag and alignment torques. This supports our hypothesis that diode rotation is caused due to the rotational torque by counterionic field.

2.4. Sideways Diode Motion and Steering on Complex Trajectories

The next challenge related to the electronic control of a self-propelling diode motion was steering it on a trajectory at a certain angle with regards to the field direction (without executing complete turnaround). We could achieve such steering control when the magnitude of the applied duty cycle is not sufficiently high

to completely rotate the diode. In this case, the diode exhibits sideways motion as shown in Figure 4a and visualized in Video V5 in the Supporting Information. As the rotational torque acting on the diode does not fully overcome the alignment torque and the viscous drag, the diode rotates only partially and moves in this direction. Interestingly, we have observed sideways motion in multiple directions for a given orientation of a partially rotated diode. Few motion trajectories observed during sideways diode motion are illustrated in Figure 4b.

We believe that this complex motion pattern is an outcome of two effects: (i) reactive propulsive force (from the counterion flux near diode surface) and (ii) rotational torque (from the counterion redistribution across wire electrodes), acting simultaneously on the diode. Further work would make possible to understand in depth how each of the interconnected electrohydrodynamic effects taking place in the water container influences the direction of sideways motion when the diode partially rotates. Additional level of control on the precise direction of diode motion could be imparted by using multielectrode setup with phase-synchronized signals and further into the future—by using self-propelling circuits with internal logic and on-board steering mechanisms.

3. Conclusions

We designed and implemented a technique that allows simple and effective on-demand steering of the self-propelling diodes by means of remotely controlling the parameters of the AC

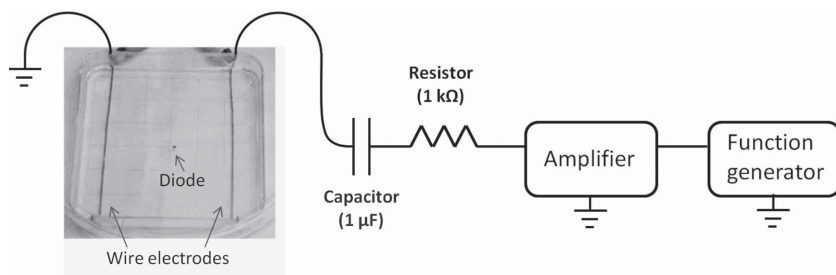


Figure 5. Schematic of the experimental setup used for applying to the wire electrodes short-duration DC component along with the AC signal. The capacitor is blocking the long-term DC component in the signal, allowing for the intermittent charge buildup, leading to torque on the diode.

electric field, which also provides them with energy. The diodes constitute a unique class of self-propelling particles since they can harvest energy from uniform external AC fields (where electrophoretic motion of other particles, if present in the system, does not occur). Application of short-lasting DC fields induces counterionic redistribution that serves as means to remotely rotate the diode. The use of such field bursts eliminates the undesirable fluid flows that would otherwise be present during the application of constant DC fields. We demonstrated previously that in addition to motion, other functionalities inherent in the microcircuit components can also be powered by the rectified signal.^[24] This unique integration of electroosmotic propellency and internal logic functions may be used in future microbots that can cooperate and communicate with each other and perform medical diagnostics and surgery.^[29,45] The self-propelling diodes can also perform motion-based sensing^[46] since their nature of motion, velocity and direction are affected by the external stimuli such as pH and surface active species.^[24] Wang et al. have already demonstrated miniaturization by self-propulsion of nanowire diodes.^[41] Their surface functionalization could in the future enable functions such as selective cargo or biomolecule pick-up/transport/delivery,^[47] writing of nanostructures,^[48] and environmental remediation.^[49]

This report introduces to the emerging field of microrobotics the ability to steer the moving microdevices and precisely control their direction of motion, which would be essential to realize all these potential applications. Even more comprehensive field-encoded means of steering and control can be applied in future self-propelling microdevices that could include a complex circuit with an on-board logic and control as envisioned in our publication describing the principle of such self-propellency.^[24] Thus, the above demonstration of remote steering of self-propelling microdevices encoded via duty cycle modulation is only one of the initial steps toward the development of “intelligent” particles and microdevices that could in the future enable practical medical and biotechnology operations, environmental monitoring or collective assembly of smart self-reconfiguring structures.

4. Experimental Section

The experiments were carried out in a plastic Petri dish of dimensions 9 cm × 9 cm × 1.5 cm in depth, with two thin wire electrodes at its bottom on opposite ends separated by a gap of 7 cm. Deionized (DI)

water (18.2 MΩ cm at 25 °C) was obtained from a Millipore Milli-Q Academic water purification system (Billerica, MA). Silicon switching microdiodes (1.3 mm × 0.9 mm × 0.65 mm, part number 1N4448HWT-DICT-ND, Digi-Key Co.) were floated on the surface of DI water contained in the Petri dish, suspended by surface tension. The water layer in the Petri dish was ≈0.5 cm thick.

The schematic of the electrical actuating and steering circuit is provided in **Figure 5**. Square-wave AC signal (800 V peak-to-peak, 1 kHz) was applied to the circuit, comprising of wire electrodes connected in series to a 1 kΩ resistor, from a function generator (Agilent, 33120 A) and amplifier (Trek, PZD 700). The signal was monitored using an oscilloscope and a digital multimeter. The wave symmetry (duty cycle) was changed digitally from the function generator. A 1 μF capacitor was added in series to the wire electrodes to induce diode rotation. The diode motion was observed under Olympus SZ-61 optical microscope and recorded with Sony DSC-V1 Cyber-Shot digital camera. The control experiment at the IEP of Petri dish was performed by lowering the pH of DI water to 5 by addition of HCl and the control experiment at the IEP of diode surface was performed by increasing the pH of DI water to 6.4 by addition of NaOH.

Supporting Information

Supporting Information is available from the Wiley Online Library or from the author.

Acknowledgements

This study was supported by the US National Science Foundation through the Research Triangle NSF MRSEC on Programmable Soft Matter (DMR-1121107) and NSF grant CBET-0828900.

Received: May 24, 2015

Revised: July 4, 2015

Published online: August 11, 2015

- [1] T. E. Mallouk, A. Sen, *Sci. Am.* **2009**, 300, 72.
- [2] J. Wang, *ACS Nano* **2009**, 3, 4.
- [3] T. Mirkovic, N. S. Zacharia, G. D. Scholes, G. A. Ozin, *ACS Nano* **2010**, 4, 1782.
- [4] S. J. Ebbens, J. R. Howse, *Soft Matter* **2010**, 6, 726.
- [5] S. Sengupta, M. E. Ibele, A. Sen, *Angew. Chem. Int. Ed.* **2012**, 51, 8434.
- [6] W. R. Browne, B. L. Feringa, *Nat. Nanotechnol.* **2006**, 1, 25.
- [7] R. Sharma, S.-T. Chang, O. D. Velev, *Langmuir* **2012**, 28, 10128.
- [8] N. Bassik, B. T. Abebe, D. H. Gracias, *Langmuir* **2008**, 24, 12158.
- [9] D. Okawa, S. J. Pastine, A. Zettl, J. M. J. Frechet, *J. Am. Chem. Soc.* **2009**, 131, 5396.
- [10] R. F. Ismagilov, A. Schwartz, N. Bowden, G. M. Whitesides, *Angew. Chem. Int. Ed.* **2002**, 41, 652.
- [11] A. A. Solovev, W. Xi, D. H. Gracias, S. M. Harazim, C. Deneke, S. Sanchez, O. G. Schmidt, *ACS Nano* **2012**, 6, 1751.
- [12] W. Gao, S. Sattayasamitsathit, K. M. Manesh, D. Weihs, J. Wang, *J. Am. Chem. Soc.* **2010**, 132, 14403.
- [13] Y. Wang, R. M. Hernandez, D. J. Bartlett, Jr., J. M. Bingham, T. R. Kline, A. Sen, T. E. Mallouk, *Langmuir* **2006**, 22, 10451.
- [14] N. Mano, A. Heller, *J. Am. Chem. Soc.* **2005**, 127, 11574.

- [15] T.-C. Lee, M. Alarcon-Correa, C. Miksch, K. Hahn, J. G. Gibbs, P. Fischer, *Nano Lett.* **2014**, *14*, 2407.
- [16] R. A. Pavlick, S. Sengupta, T. McFadden, H. Zhang, A. Sen, *Angew. Chem. Int. Ed.* **2011**, *50*, 9374.
- [17] J. R. Howse, R. A. L. Jones, A. J. Ryan, T. Gough, R. Vafabakhsh, R. Golestanian, *Phys. Rev. Lett.* **2005**, *99*, 048102.
- [18] R. Yoshida, *Adv. Mater.* **2010**, *22*, 3463.
- [19] S. Maeda, Y. Hara, T. Sakai, R. Yoshida, S. Hashimoto, *Adv. Mater.* **2007**, *19*, 3480.
- [20] D. Pantarotto, W. R. Browne, B. L. Feringa, *Chem. Commun.* **2008**, *13*, 1533.
- [21] R. K. Soong, G. D. Bachand, H. P. Neves, A. G. Olkhovets, H. G. Craighead, C. D. Montemagno, *Science* **2000**, *290*, 1555.
- [22] G. Loget, A. Kuhn, *Nat. Commun.* **2011**, *2*, 535.
- [23] G. H. Kwon, J. Y. Park, J. Y. Kim, M. L. Frisk, D. J. Beebe, S. H. Lee, *Small* **2008**, *4*, 2148.
- [24] S. T. Chang, V. N. Paunov, D. N. Petsev, O. D. Velev, *Nat. Mater.* **2007**, *6*, 235.
- [25] R. Dreyfus, J. Baudry, M. L. Roper, M. Fermigier, H. A. Stone, J. Bibette, *Nature* **2005**, *437*, 862.
- [26] P. Fischer, A. Ghosh, *Nanoscale* **2011**, *3*, 557.
- [27] W. Wang, L. A. Castro, M. Hoyos, T. E. Mallouk, *ACS Nano* **2012**, *6*, 6122.
- [28] D. Kagan, M. J. Benichmol, J. C. Claussen, E. Chuluun-Erdene, S. Esener, J. Wang, *Angew. Chem. Int. Ed.* **2012**, *51*, 7519.
- [29] J. Wang, W. Gao, *ACS Nano* **2012**, *6*, 5745.
- [30] D. Patra, S. Sengupta, W. Duan, H. Zhang, R. Pavlick, A. Sen, *Nanoscale* **2013**, *5*, 1273.
- [31] D. Kagan, R. Laocharoensuk, M. Zimmerman, C. Clawson, S. Balasubramanian, D. Kang, D. Bishop, S. Sattayasamitsathit, L. Zhang, J. Wang, *Small* **2010**, *6*, 2741.
- [32] A. A. Solovev, S. Sanchez, M. Pumera, Y. F. Mei, O. G. Schmidt, *Adv. Funct. Mater.* **2010**, *20*, 2430.
- [33] Y. Y. Hong, M. Diaz, U. M. Cordova-Figueroa, A. Sen, *Adv. Funct. Mater.* **2010**, *20*, 1568.
- [34] S. Campuzano, D. Kagan, J. Orozco, J. Wang, *Analyst* **2011**, *136*, 4621.
- [35] W. Yang, V. R. Misko, K. Nelissen, M. Kongd, F. M. Peeters, *Soft Matter* **2012**, *8*, 5175.
- [36] D. R. Frutiger, B. E. Kratochvil, K. Vollmers, B. J. Nelson, *IEEE Int. Conf. Rob.* **2008**, *1-9*, 1770.
- [37] Y. Y. Hong, D. Velegol, N. Chaturvedi, A. Sen, *Phys. Chem. Chem. Phys.* **2010**, *12*, 1423.
- [38] M. Guix, J. Orozco, M. Garcia, W. Gao, S. Sattayasamitsathit, A. Merkoci, A. Escarpa, J. Wang, *ACS Nano* **2012**, *6*, 4445.
- [39] V. Magdanz, G. Stoychev, L. Ionov, S. Sanchez, O. G. Schmidt, *Angew. Chem. Int. Ed.* **2014**, *126*, 2711.
- [40] S. T. Chang, E. Beaumont, D. N. Petsev, O. D. Velev, *Lab Chip* **2008**, *8*, 117.
- [41] P. Calvo-Marzal, S. Sattayasamitsathit, S. Balasubramanian, J. R. Windmiller, C. Dao, J. Wang, *Chem. Commun.* **2010**, *46*, 1623.
- [42] J. Roche, S. Carrara, J. Sanchez, J. Lannelongue, G. Loget, L. Bouffier, P. Fischer, A. Kuhn, *Sci. Rep.* **2014**, *4*, 6705.
- [43] T. B. Jones, in *Electromechanics of Particles*, Cambridge University Press, NY **1995**, Ch. 5.
- [44] J. N. Israelachvili, in *Intermolecular and Surface Forces*, Academic Press, MA **2011**, Chs. 4, 14.
- [45] B. J. Nelson, I. K. Kaliakatsos, J. J. Abbott, *Annu. Rev. Biomed. Eng.* **2010**, *12*, 55.
- [46] D. Kagan, P. Calvo-Marzal, S. Balasubramanian, S. Sattayasamitsathit, K. M. Manesh, G.-U. Flechsig, J. Wang, *J. Am. Chem. Soc.* **2009**, *131*, 12082.
- [47] J. Wang, *Lab Chip* **2012**, *12*, 1944.
- [48] K. M. Manesh, S. Balasubramanian, J. Wang, *Chem. Commun.* **2010**, *46*, 5704.
- [49] W. Gao, J. Wang, *ACS Nano* **2014**, *8*, 3170.